



OPEN ACCESS

EDITED BY

Dahlia Zaidel,
University of California, Los Angeles,
United States

REVIEWED BY

Xinyuan Yan,
University of Minnesota Twin Cities,
United States
Ilaria Marcantoni,
Marche Polytechnic University, Italy

*CORRESPONDENCE

Silvia Savazzi
✉ silvia.savazzi@univr.it

RECEIVED 28 December 2023

ACCEPTED 23 February 2024

PUBLISHED 07 March 2024

CITATION

Mazzi C, Mele S, Bagattini C, Sanchez-Lopez J and Savazzi S (2024) Coherent activity within and between hemispheres: cortico-cortical connectivity revealed by rTMS of the right posterior parietal cortex.
Front. Hum. Neurosci. 18:1362742.
doi: 10.3389/fnhum.2024.1362742

COPYRIGHT

© 2024 Mazzi, Mele, Bagattini, Sanchez-Lopez and Savazzi. This is an open-access article distributed under the terms of the [Creative Commons Attribution License \(CC BY\)](https://creativecommons.org/licenses/by/4.0/). The use, distribution or reproduction in other forums is permitted, provided the original author(s) and the copyright owner(s) are credited and that the original publication in this journal is cited, in accordance with accepted academic practice. No use, distribution or reproduction is permitted which does not comply with these terms.

Coherent activity within and between hemispheres: cortico-cortical connectivity revealed by rTMS of the right posterior parietal cortex

Chiara Mazzi¹, Sonia Mele¹, Chiara Bagattini^{1,2},
Javier Sanchez-Lopez³ and Silvia Savazzi ^{1*}

¹Perception and Awareness (PandA) Laboratory, Department of Neuroscience, Biomedicine and Movement Sciences, University of Verona, Verona, Italy, ²Section of Neurosurgery, Department of Neuroscience, Biomedicine and Movement Sciences, University of Verona, Verona, Italy, ³Escuela Nacional de Estudios Superiores Unidad Juriquilla, Universidad Nacional Autonoma de Mexico, Santiago de Querétaro, Mexico

Introduction: Low frequency (1 Hz) repetitive transcranial stimulation (rTMS) applied over right posterior parietal cortex (rPPC) has been shown to reduce cortical excitability both of the stimulated area and of the interconnected contralateral homologous areas. In the present study, we investigated the whole pattern of intra- and inter-hemispheric cortico-cortical connectivity changes induced by rTMS over rPPC.

Methods: To do so, 14 healthy participants underwent resting state EEG recording before and after 30 min of rTMS at 1 Hz or sham stimulation over the rPPC (electrode position P6). Real stimulation was applied at 90% of motor threshold. Coherence values were computed on the electrodes nearby the stimulated site (i.e., P4, P8, and CP6) considering all possible inter- and intra-hemispheric combinations for the following frequency bands: delta (0.5–4 Hz), theta (4–8 Hz), alpha (8–12 Hz), low beta (12–20 Hz), high beta (20–30 Hz), and gamma (30–50 Hz).

Results and discussion: Results revealed a significant increase in coherence in delta, theta, alpha and beta frequency bands between rPPC and the contralateral homologous sites. Moreover, an increase in coherence in theta, alpha, beta and gamma frequency bands was found between rPPC and right frontal sites, reflecting the activation of the fronto-parietal network within the right hemisphere. Summarizing, subthreshold rTMS over rPPC revealed cortico-cortical inter- and intra-hemispheric connectivity as measured by the increase in coherence among these areas. Moreover, the present results further confirm previous evidence indicating that the increase of coherence values is related to intra- and inter-hemispheric inhibitory effects of rTMS. These results can have implications for devising evidence-based rehabilitation protocols after stroke.

KEYWORDS

resting state, EEG oscillatory dynamics, functional connectivity, inter-hemispheric coherence, rTMS

1 Introduction

Repetitive transcranial magnetic stimulation (rTMS) is a non-invasive method to temporarily modulate neural activity (Silvanto and Muggleton, 2008; Miniussi et al., 2013) with long-lasting changes of cortical excitability (Robertson et al., 2003). Importantly, rTMS not only acts locally on interneural circuits underneath the coil but its effects

also spread to functionally connected brain regions along cortico-cortical connections (Bortoletto et al., 2015; Siviero et al., 2023). When TMS is coupled with EEG, it is possible to map the network of cortical areas engaged in a specific cognitive function and give information on the functional coupling among brain areas with a very high temporal resolution (Ilmoniemi et al., 1997; Miniussi and Thut, 2010) thus providing information on the causal role of TMS-induced cortical changes on distant, but functionally interconnected, areas. The advantage of recording EEG before and after the delivery of a rTMS protocol is that of potentially providing information on the causal relationship between functionally connected areas in terms of both the temporal dynamics (pre- vs. post-stimulation) and the nature (excitatory vs. inhibitory) of the signal that is spread. That is, if an area A is active prior to area B, it can be assumed that area A and B are functionally connected, because a change in area A has an effect on area B, and that activity in area A causes a change in the activity of area B. Moreover, if area A, as an example, is inhibited by rTMS and a coherent reduction of activity is found in area B, the two areas are positively connected (i.e., excitatory connection), conversely if a reduction of activity in area A is followed by an enhancement of activity in area B, the two areas are negatively (i.e., inhibitory connection) connected (Miniussi and Thut, 2010).

Importantly, EEG can provide useful information in terms of brain oscillations which are a notable feature of brain activity and they are thought to play a central role in cognition (Wang, 2010; Tafuro et al., 2023). EEG signal can indeed be decomposed into frequency bands (Berger, 1929), each of which showing a specific power reflecting the amount of synchronized oscillatory activity expressed by neuronal ensembles oscillating in that specific frequency band. Importantly, the power of each frequency band can be used to calculate coherence, i.e., a measure reflecting the strength and the sign of the interplay between patterns of oscillating brain activity recorded at different locations on the scalp, and it is suggested to sustain effective communication among groups of neurons (Fries, 2005). Thus, high coherence between EEG signals recorded at different electrodes suggests high functional coupling between the underlying neuronal networks (i.e., functional connectivity). Coherence can be measured while participants are not performing any task (resting state) and it can, thus, reveal functional connectivity of areas in the resting state. Moreover, if resting state coherence is recorded prior and after the application of a rTMS protocol, it can give important insights on rTMS-induced perturbation effects on the state of the cortex in different areas of the brain, thus revealing both the network(s) of areas functionally connected with the stimulated site and the nature (excitatory vs. inhibitory) of this functional coupling. That is, if coherence among two sites is increased after inhibition of one of the two, it reflects an excitatory connection between the two sites (i.e., both sites are inhibited), conversely if coherence is decreased after the inhibition of one of the two, it reflects an inhibitory connection between the two sites (one site is inhibited and the other is excited).

From a translational perspective, the possibility to detect changes at the network level by means of measures of coherence in brain networks can pave the way for the development of effective interventions aimed at restoring cognitive deficits in stroke patients. Indeed, low-frequency rTMS of the right (contralesional)

frontal cortex has been shown to reduce non-fluent aphasia symptoms (Shah et al., 2013), whereas low-frequency rTMS of the left (contralesional) parietal cortex has been shown to reduce symptoms (Hesse et al., 2011; Oliveri, 2011; Müri et al., 2013) in spatial neglect, i.e., a failure to report, respond, or orient to stimuli presented to the contralesional space (Heilman and Valenstein, 1979; Schenkenberg et al., 1980; Savazzi et al., 2007). The logic underlying the application of rTMS on the contralesional hemisphere stands on the assumptions of the interhemispheric rivalry model (Kinsbourne, 1977) stating that, in normal conditions, the two hemispheres inhibit each other. Accordingly, after a lesion to one hemisphere, the contralesional hemisphere is released from the inhibition exerted by the damaged one and becomes hyperactive. However, despite several pieces of evidence showing the efficacy of rTMS in restoring cognitive functions, little is known about the neural underpinnings allowing this to occur and different mechanisms are proposed for the amelioration of symptoms in aphasia and neglect patients. In this respect, amelioration of neglect symptoms, by applying rTMS to the contralesional hemisphere, has been invariably explained in terms of a reduction of the hyperactivity of the undamaged hemisphere and a restoration of the interhemispheric balance (Jacquin-Courtois, 2015). Conversely, amelioration of aphasia symptoms has been interpreted both as a restoration of the interhemispheric balance and as a reduction of maladaptive activation of areas within the right hemisphere (Gainotti, 2015). Importantly, most of the studies showing hyperactivity of the contralesional hemisphere in patients with neglect refers to sub-acute or chronic patients and, thus, leaving open the possibility, as proposed in aphasia literature, that the hyperactivity of the contralesional hemisphere might be the result of maladaptive plasticity (Umarova et al., 2011; Pia et al., 2012; Ricci et al., 2012; Bagattini et al., 2015b) as opposed to a release from inhibition caused by a lesion. Thus, understanding the role of the non-lesioned hemisphere in the genesis and maintenance of the deficits is important not only for a better comprehension of the neural plasticity and reorganization after stroke, but it will be crucial for devising more effective rehabilitation protocols (Bartolomeo, 2014; Lunven et al., 2015).

Several attempts to understand the interplay between the hemispheres to uncover the effects of hypo-activity (due to a lesion or caused by low frequency, inhibitory, rTMS) in one hemisphere on the functionality of the other (i.e., induced hyper-activation or hypo-activation) have been made (e.g., Koch et al., 2008, 2011, 2013; Salatino et al., 2014). However, none of them have used a direct approach by investigating coherence among brain areas with inhibitory TMS approaches for areas different from motor ones (e.g., Strens et al., 2002; Chen et al., 2003). To the best of our knowledge, such an approach to directly test the hypothesis that a reduction of activity in one hemisphere (right parietal lobe) would result in an enhancement of activity in homologous areas in the other hemisphere was present only in a paper by Bagattini et al. (2015b). In this paper, the authors applied 1 Hz rTMS in healthy participants to reduce cortical reactivity in one hemisphere and concurrently measured, with EEG, the effects of this reduction in functionally connected areas. They found that the sites contralateral to the stimulation exhibited a reduction in activity similar to that induced in the stimulated hemisphere. Similarly, adopting an

interleaved TMS-fMRI approach, Ricci et al. (2012) showed that low frequency rTMS over right posterior parietal cortex (rPPC) caused decreased neural activity of parieto-frontal regions and of the homologous parietal regions of the left hemisphere. These results were, thus, in direct contrast to the hypothesis of a reciprocal inhibition of the two hemispheres suggesting that what is proposed for aphasia, i.e., maladaptive plasticity, could also account for spatial neglect.

Here, we extend previous investigations by means of an inhibitory rTMS protocol applied over rPPC and by recording resting state EEG before and after the application of rTMS. Coherence between the stimulated site and other cortical areas is used as a measure of functional connectivity to reveal both the functionally interconnected networks engaged by the stimulation and the nature of this connection. The aim of the present paper is, thus, that of revealing whether the reduction of cortical activity induced by 1 Hz rTMS in one hemisphere leads to a reduction (high coherence) of neural activity in other areas within the same hemisphere or on the contralateral hemisphere, thus providing evidence on cortico-cortical connectivity between rPPC and other brain areas. Implications for possible recruitment of intra- and inter-hemispheric neural pathways in spatial neglect are discussed.

2 Materials and methods

2.1 Participants

Twenty-one right-handed (as assessed with the Edinburgh Handedness Inventory; Oldfield, 1971) healthy volunteers (14 females), aged 19–33 years (mean 24.81 years, sd 3.39 years), took part in the experiment. They all had normal or corrected-to-normal visual acuity and no history of neurological or psychiatric disorders. All gave their written informed consent to participate in the experiment. The experiment was carried out according to the principles laid down in the 2013 Declaration of Helsinki and approved by the local Ethics Committee. The data from seven participants were not included in the analysis because of high noise in the EEG recordings or a too low number of segments for the power and coherence analysis (see below). Therefore, the research sample consisted of 14 participants (nine females; mean age 24.71 years, sd 3.41 years).

As assessed by a safety screening questionnaire (adapted from Rossi et al., 2011), the participants were negative for all the risk factors associated with TMS: none reported neurological disorders, cardiac pacemaker, any history of epilepsy or migraine, current treatment with any psychoactive medication or pregnancy.

2.2 Experimental design

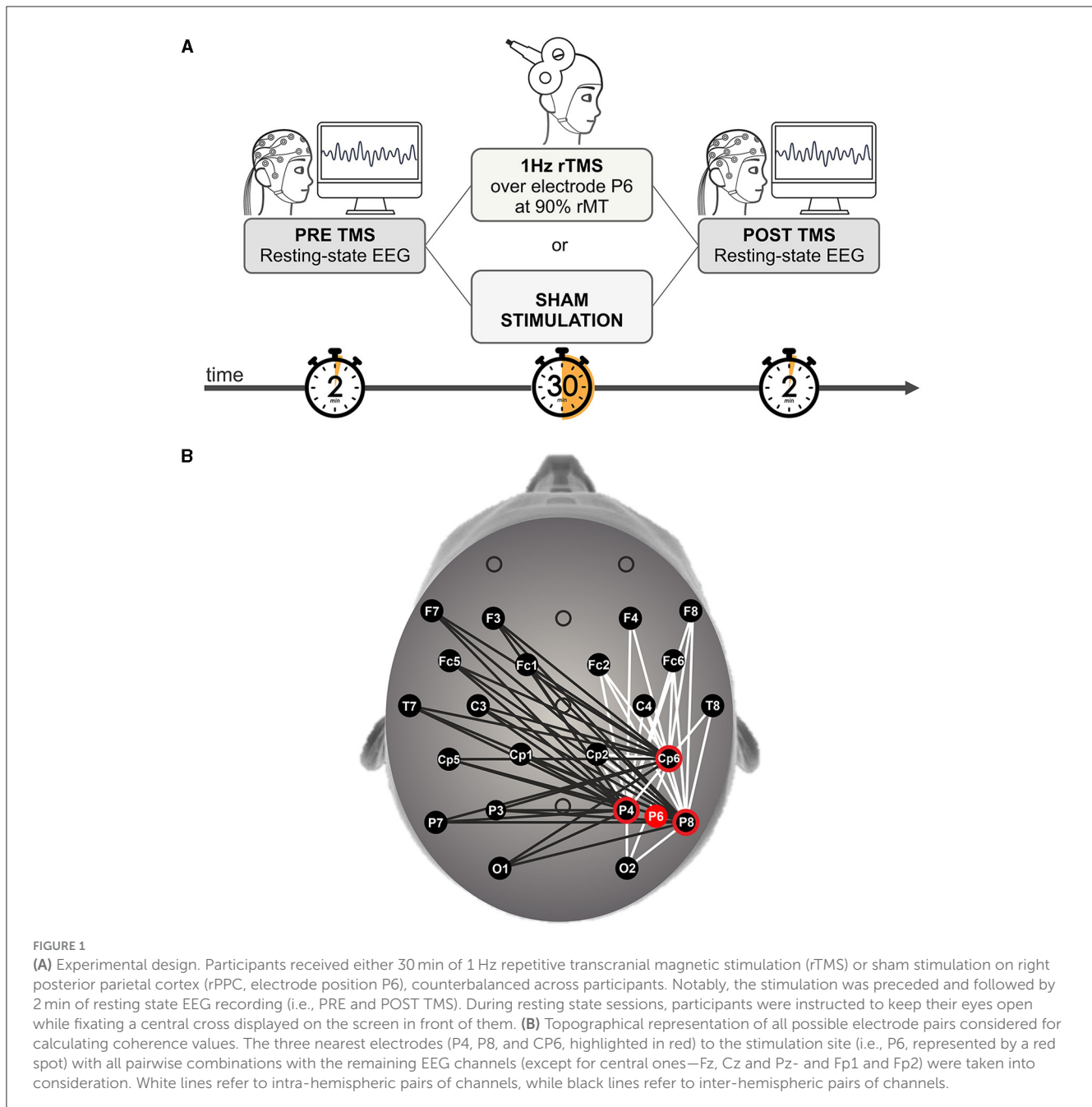
Figure 1A illustrates the experimental design. Two experimental sessions (TMS/Sham), the order of which was counterbalanced across participants, were conducted on two separate days. The sequence of each of the two experimental sessions was as the following. After placing the cap with electrodes for EEG recording, the motor threshold was assessed at the beginning of the first session to set the stimulation intensity (see

TMS protocol section). Two minutes of resting-state EEG activity were then recorded, immediately before and after (hereafter called “PRE” and “POST”) the main stimulation protocols (TMS or Sham), which lasted for 30 min. Participants were tested in a dimly lit room, seated in a comfortable chair with their head stabilized by a chinrest and their eyes open while watching a fixation cross at the center of a black computer screen positioned at a viewing distance of about 57 cm.

In order to reduce uncontrolled effects of “mind wandering” or non-specific brain activity related to thoughts or mental imagery, which could affect the ongoing activity in the targeted systems and associated networks (Silvanto and Muggleton, 2008), the participants were instructed to relax and free their mind both during resting EEG recordings and stimulation. This procedure was adopted in both the stimulation protocols (TMS/Sham) to render all the protocols homogeneous with respect to the instructions.

2.3 TMS protocol

rTMS was delivered through a 70 mm figure-of-eight Magstim Air Film Coil connected with a Magstim Rapid² system (maximum output 3.5 Tesla) (Magstim Company Limited, Whitland, UK). The stimulation was delivered at 1 Hz for 30 min (total number of pulses = 1,800) at 90% (mean 54.93% of Maximum Stimulator Output, MSO) of resting motor threshold (mean 61% of the MSO). These parameters have been shown to have an inhibitory effect on the stimulated cortex, that is to reduce cortical excitability for several minutes beyond the duration of the TMS trains (Maeda et al., 2000; Valero-Cabré et al., 2006; Bagattini et al., 2015b). Motor threshold was measured as the minimum stimulation intensity able to elicit a motor evoked potential (MEP) of ≥ 50 μ V in the left first dorsal interosseous muscle in five of ten consecutive stimulations (Rossini et al., 1994). rTMS was applied unilaterally over the right posterior parietal cortex (rPPC) between P4 and P8 electrodes of the 10–20 International EEG system (i.e., at the position of the P6 electrode), corresponding to the right inferior parietal lobe (Fierro et al., 2000; Brighina et al., 2002; Bagattini et al., 2015b), that is the area mostly involved in the emergence of spatial neglect and, if stimulated with TMS, capable of inducing neglect-like symptoms in healthy individuals. The TMS coil was placed tangentially to the target scalp site with the handle pointing backwards, so as to induce a posterior-to-anterior current direction in the underlying cortical surface. To stabilize the coil in the targeted position and orientation with respect to the scalp, a mechanical arm (Magstim Articulated Coil Stand) was used, and the participants wore a custom-made collar for the entire duration of the stimulation protocol preventing any head movements. Moreover, the position of the coil was constantly checked by the experimenter and, on the rare occasions it was needed, corrected. The stimulation protocol (stimulus intensity, frequency and duration of the pulse train) was selected according to the international safety guidelines (Rossi et al., 2009) and commercial earplugs were used to protect the participants from the noise associated with TMS (Rossi et al., 2009). None of the participants reported negative effects during or after stimulation. For the Sham condition, we used the same parameters as for the rTMS session but, in order to reduce the intensity of the



magnetic field reaching the scalp (Stokes et al., 2005), a custom-made 3-cm-thick block of polystyrene was placed between the coil and the scalp, thus, ensuring that the Sham stimulation was ineffective (Bagattini et al., 2015a; Mazzi et al., 2017).

2.4 EEG recording and preprocessing

TMS-compatible EEG equipment (BrainAmp, Brain Products GmbH, Munich, Germany) was used to record spontaneous EEG (BrainVision Recorder) in resting-state. EEG activity was continuously recorded from a Fast'n Easy cap with 27 TMS-compatible Ag/AgCl pellet pin electrodes (EasyCap GmbH,

Herrsching, Germany) placed according to the 10-20 International System (O1, O2, P7, P3, Pz, P4, P8, CP5, CP1, CP2, CP6, T7, C3, Cz, C4, T8, FC5, FC1, FC2, FC6, F7, F3, Fz, F4, F8, Fp1, Fp2). Additional electrodes were used as reference, ground and for the electro-oculogram. The ground electrode was placed in AFz. All scalp channels were online referenced to the right mastoid (RM) and then re-referenced offline to the average of the RM and left mastoid (LM). Horizontal and vertical eye movements were recorded, respectively, with electrodes placed at the left and right canthi and above and below the right eye. The impedance of all the electrodes was kept below 5 K Ω . The EEG was recorded at 5,000 Hz sampling rate with a time constant of 10 s as low cut-off and a high cut-off of 1,000 Hz. The EEG signal was processed and analyzed off-line using Brain Vision Analyzer 2.1.

Continuous resting-state data were off-line down-sampled to 500 Hz. Brain components corresponding to ocular artifacts (such as eye blinks and eye movements) were identified and corrected using the ICA ocular correction (restricted Infomax) algorithm implemented in Brain Vision Analyzer 2 applied over to the whole continuous signal. Following ocular correction, data were filtered with a 0.5 Hz high-pass filter with a 24 dB/octave roll-off, as well as with a notch filter to remove power line noise (50 Hz). Segmentation into non-overlapping windows of 2,048 s was then applied to all channels (Kam et al., 2013) and epochs containing artifacts were rejected before further processing by means of a semiautomatic procedure. The length of the epoch was chosen to maintain consistency with previous literature (e.g., Wacker et al., 2009; Jamieson and Burgess, 2014; Ranlund et al., 2014; Ambrosini et al., 2020; Neuhaus et al., 2021; Grieder and Koenig, 2023) and, thus, allowing for easier comparison and integration of findings across studies. Moreover, the length of 2,048 ms allows for capturing multiple cycles of lower-frequency brain oscillations, provides a sufficient time window to analyze their dynamics accurately and it is an appropriate balance between temporal resolution and statistics. That is, it is short enough to capture rapid changes in brain activity, yet long enough to reduce noise and obtain more reliable estimates of brain activity features. Subsequently, a surface Laplacian transform was performed (reference-free current source density—CSD, Nunez et al., 1997) using spherical spline interpolation (Perrin et al., 1989). Only participants with at least 25 epochs per conditions, i.e., more than 50 s (Kam et al., 2013), were included in the subsequent analyses. Notably, no significant differences (all $p > 0.05$) in the average duration of artifact-free EEG data were found across conditions (pre TMS: $M = 87$ s, $SD = 19.85$, post TMS: $M = 86$ s, $SD = 22.11$, pre SHAM: $M = 84$ s, $SD = 26.11$, post SHAM: $M = 83$ s, $SD = 19.56$).

2.5 Power

EEG power spectrum was estimated for all frequency bins between 0.5 and 50 Hz using *Fast Fourier Transform* (FFT, resolution 0.5 Hz, *Hanning window 10%*) and then averaged across epochs under the same conditions for all electrodes. Mean absolute power was then calculated for the following frequency bands: delta (0.5–4 Hz), theta (4–8 Hz), alpha (8–12 Hz), low beta (12–20 Hz), high beta (20–30 Hz) and gamma (30–50 Hz).

Regional power changes were determined using the Stimulation-Related Power (SRPow) for each condition (TMS/Sham) and each electrode position according to the following Equation (1):

$$\text{SRPow}_x(\%) = [(\text{POST Pow}_x - \text{PRE Pow}_x) / \text{PRE Pow}_x] \times 100 \quad (1)$$

Therefore, the so calculated SRPow of an electrode “x” represents the percentage change of spectral power after the stimulation (i.e., POST) when compared to a baseline (i.e., PRE, data collected before the stimulation) at a certain frequency band. As a consequence, increases in power from the baseline (i.e., PRE) to the POST stimulation phase correspond to a

positive value, whereas negative values reflect decreases in power. This event-related desynchronization/synchronization procedure (Pfurtscheller and Lopes da Silva, 1999) allowed to reduce the effects of inter-subject variability in absolute spectral power values (Gerloff et al., 1998; Hummel et al., 2002).

2.6 Coherence

EEG absolute power spectra were then used to calculate coherence. Coherence between two EEG signals (x and y) at each frequency f was then computed with BrainVision Analyzer 2 according to the following Equation (2), which represents an extension of the Pearson’s correlation coefficient to complex number pairs:

$$\text{Coh}_{xy}(f) = |\text{CS}_{xy}(f)|^2 / [|\text{CS}_{xx}(f)| |\text{CS}_{yy}(f)|] \quad (2)$$

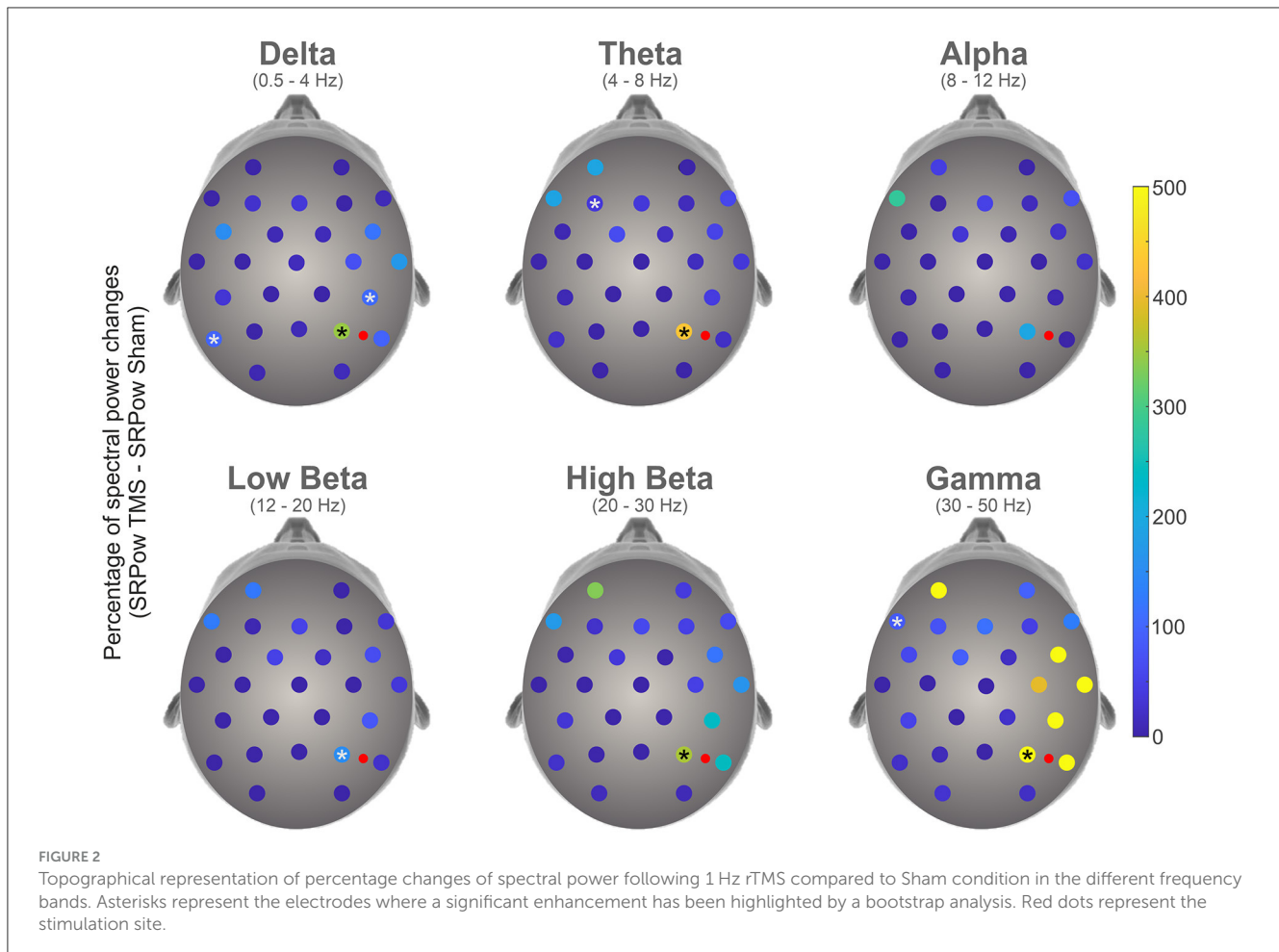
Here $\text{CS}_{xy}(f)$ corresponds to the cross-spectrum, while $\text{CS}_{xx}(f)$ and $\text{CS}_{yy}(f)$ are the autospectrum estimates of the x and y signals, respectively. Accordingly, the coherence value results in a number ranging between 0 and 1, with 0 indicating the lack of functional connectivity between two signals at a given frequency band, and 1 meaning a strong interregional interaction. Coherence values (see [Supplementary material](#)) were then pooled into the same frequency band defined as follows: delta (0.5–4 Hz), theta (4–8 Hz), alpha (8–12 Hz), low beta (12–20 Hz), high beta (20–30 Hz), and gamma (30–50 Hz).

In order to test for changes in connectivity induced by rTMS, the calculation of coherence was performed by considering the three nearest electrodes to the stimulation site (i.e., P4, P8, CP6) with all possible intra- and inter-hemispheric combinations (Figure 1B). Specifically, intra-hemispheric coherence (namely, within the stimulated hemisphere) was assessed on the right hemisphere considering the electrodes of interest in combination with O2, CP2, T8, C4, FC6, FC2, F8, and F4. Similarly, inter-hemispheric coherence (namely, reflecting functional connectivity between the stimulated site and the contralateral hemisphere) was assessed considering the same three electrodes of interest in combination with O1, P7, P3, CP5, CP1, T7, C3, FC5, FC1, F7, and F3 (all placed on the left hemisphere).

Stimulation-Related Coherence (SRCoh, Plewnia et al., 2008) was then calculated for each stimulation condition (TMS and Sham) by means of the Equation (3):

$$\text{SRCoh}_{xy} = \text{POST Coh}_{xy} - \text{PRE Coh}_{xy} \quad (3)$$

Therefore, positive values indicate a stronger coherence as a consequence of the stimulation protocol. Conversely, SRCoh has a negative value when coherence is lower after the stimulation than before. The present procedure has, thus, the dual advantage of (1) normalizing for the effect of the baseline coherence level and (2) reducing the effect of inter-subject and inter-electrode variability of absolute spectral coherence introduced by the reference electrodes (Fein et al., 1988; Rappelsberger and Petsche, 1988).



2.7 Statistical analysis

Statistical comparisons between conditions were performed on SRPow and SRCoh values using a series of one-tailed paired *t*-tests with bootstrapping in order to reveal reliable increments of these measures after rTMS compared to Sham.

Specifically, as far as concerns power, rTMS SRPow values for each electrode were compared to Sham SRPow values in all investigated frequency bands (δ , θ , α , low β , high β , γ). Taking into account coherence, rTMS SRCoh values were compared to Sham SRCoh values in all the considered frequency bands. The difference in SRPow and SRCoh values for the two stimulation conditions (rTMS/Sham) was analyzed by means of a non-parametric Monte Carlo percentile bootstrap simulation (Efron and Tibshirani, 1993; Oruç et al., 2011) implemented into a custom-made Matlab (MathWorks, Natick, MA) script. This procedure creates a simulated data distribution by re-sampling the data with replacement. To this end, 50,000 re-samples for the rTMS minus Sham conditions of both SRPow and SRCoh values were used. The lower 5th percentile of the re-sampled data distribution served as the critical values for the one-tailed 0.05 significance level. If the 5th percentile results to be above the zero level (rTMS > Sham), it means that values of SRPow and SRCoh are significantly larger for the rTMS condition than the Sham condition. This analysis was performed separately for SRPow and SRCoh values,

electrode/electrode pairs (see Figure 1B) and frequency bands (δ , θ , α , low β , high β , γ).

3 Results

3.1 Power

Figure 2 represents the increment of SRPow after rTMS compared to Sham, for each electrode as a function of the frequency bands. Bootstrap analysis revealed a significant enhancement of power (in percentage of change) following rTMS compared to Sham condition in electrodes P4 (345.88, $p < 0.0001$), CP6 (106.95, $p < 0.0001$) and P7 (98.76, $p < 0.0001$) in Delta band, P4 (430.81, $p < 0.0001$) and F3 (36.79, $p < 0.0001$) in Theta, P4 in both Low (153.90, $p < 0.0001$) and High (355.96, $p < 0.0001$) Beta and P4 (499.07, 0.0001) and F7 (84.56, $p < 0.0001$) in Gamma domain. Statistical analysis did not yield any significant differences in the alpha band.

3.2 Coherence

Statistical results for intra- and inter-hemispheric coherence are, respectively, reported in Tables 1 and 2 as assessed by bootstrap

TABLE 1 Results of the bootstrap analysis comparing rTMS SRCoh vs. Sham SRCoh condition concerning intra-hemispheric coherence data.

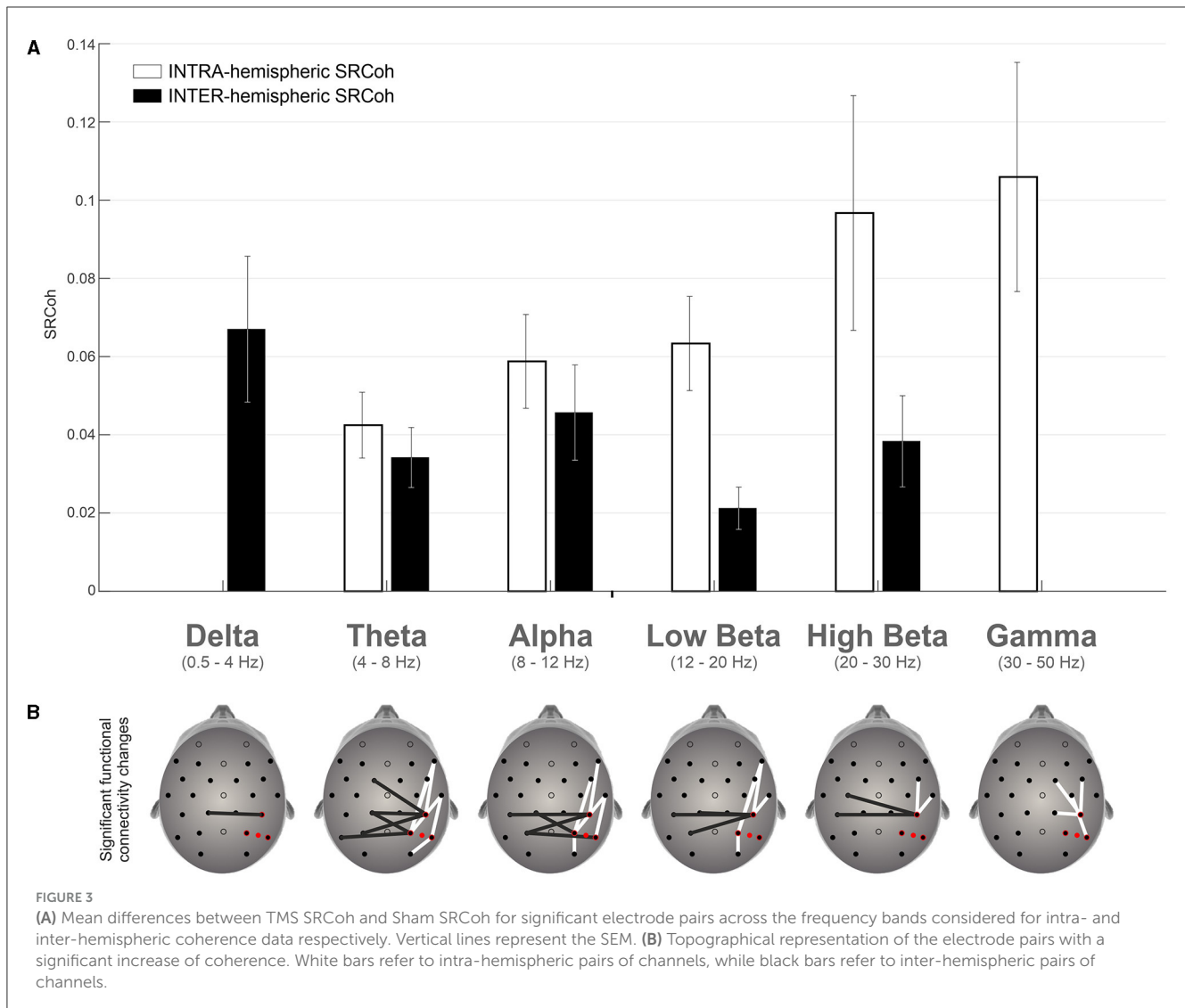
Intra-hemispheric coherence	O2	CP2	T8	C4	FC6	FC2	F8	F4
Delta (0.5–4 Hz)								
P4	0.043	0.003	0.011	0.002	0.003	−0.017	0.014	0.027
	0.18	0.48	0.28	0.48	0.45	0.80	0.27	0.07
P8	0.010	0.026	0.021	0.008	−0.039	0.004	−0.005	0.005
	0.35	0.19	0.17	0.41	0.85	0.45	0.55	0.47
CP6	−0.012	0.035	0.023	0.058	−0.005	0.025	0.001	0.031
	0.58	0.22	0.18	0.14	0.60	0.17	0.47	0.10
Theta (4–8 Hz)								
P4	0.035	0.029	0.028	0.019	0.051	0.011	0.060	0.020
	0.14	0.10	0.04	0.13	0.02	0.20	0.01	0.16
P8	0.030	0.009	0.052	0.009	−0.008	−0.010	0.016	0.002
	0.04	0.34	0.0001	0.30	0.71	0.78	0.23	0.44
CP6	−0.012	0.019	0.011	0.038	0.005	0.002	0.034	−0.002
	0.74	0.17	0.34	0.13	0.36	0.45	0.046	0.59
Alpha (8–12 Hz)								
P4	0.072	0.039	0.044	0.026	0.066	−0.016	0.073	0.011
	0.03	0.08	0.04	0.16	0.01	0.67	0.01	0.33
P8	0.030	0.018	0.055	0.022	0.022	0.009	−0.003	0.014
	0.24	0.35	0.04	0.29	0.28	0.38	0.56	0.24
CP6	0.030	0.028	0.049	0.021	0.029	0.004	0.056	−0.021
	0.17	0.21	0.10	0.32	0.19	0.45	0.02	0.79
Low beta (12–20 Hz)								
P4	0.029	−0.014	0.014	0.009	0.038	−0.011	0.069	0.018
	0.03	0.75	0.31	0.32	0.01	0.61	0.001	0.19
P8	0.045	0.022	0.108	0.061	0.053	0.025	−0.011	0.040
	0.14	0.25	0.07	0.14	0.14	0.11	0.60	0.11
CP6	0.043	0.035	0.104	0.060	0.061	−0.004	0.077	0.038
	0.13	0.10	0.01	0.15	0.10	0.59	0.004	0.14
High beta (20–30 Hz)								
P4	0.050	0.019	0.022	0.054	0.047	0.012	0.073	0.012
	0.11	0.26	0.37	0.12	0.11	0.31	0.10	0.36
P8	0.072	0.049	0.122	0.087	0.054	0.028	0.049	0.038
	0.12	0.14	0.05	0.05	0.20	0.13	0.23	0.19
CP6	0.068	0.058	0.107	0.071	0.087	0.025	0.071	0.026
	0.09	0.07	0.03	0.09	0.04	0.16	0.07	0.22
Gamma (30–50 Hz)								
P4	0.039	0.059	0.023	0.067	0.022	0.065	0.094	0.013
	0.28	0.10	0.39	0.11	0.34	0.05	0.06	0.40
P8	0.071	0.070	0.070	0.091	0.066	0.048	0.030	0.027
	0.16	0.10	0.20	0.048	0.11	0.12	0.33	0.26
CP6	0.083	0.132	0.095	0.085	0.102	0.098	0.072	0.026
	0.11	0.01	0.096	0.11	0.03	0.02	0.06	0.28

The value above in each cell corresponds to the difference between rTMS SRCoh and Sham SRCoh while the value below refers to the exact *p*-value obtained. Significant results are highlighted in red bold font.

TABLE 2 Results of the bootstrap analysis comparing rTMS SRCoh vs. Sham SRCoh condition concerning inter-hemispheric coherence data.

Inter-hemispheric coherence	O1	P7	P3	CP5	CP1	T7	C3	FC5	FC1	F7	F3
Delta (0.5–4 Hz)											
P4	−0.010	0.000	0.049	−0.014	0.051	−0.048	0.006	−0.043	0.010	0.018	0.007
	0.55	0.48	0.12	0.66	0.10	0.97	0.48	0.89	0.36	0.38	0.41
P8	0.018	0.007	0.016	0.010	0.038	−0.019	0.008	0.002	−0.033	−0.005	−0.01
	0.23	0.43	0.27	0.37	0.07	0.77	0.40	0.48	0.84	0.55	0.61
CP6	−0.029	0.031	0.025	0.046	0.067	−0.043	0.031	−0.027	−0.017	0.002	−0.006
	0.67	0.24	0.31	0.15	0.01	0.79	0.26	0.65	0.84	0.48	0.50
Theta (4–8 Hz)											
P4	0.020	0.027	0.042	0.017	0.046	0.000	0.030	−0.029	0.013	0.017	0.001
	0.27	0.01	0.06	0.17	0.0004	0.51	0.18	0.77	0.21	0.33	0.46
P8	−0.003	0.020	0.017	0.015	−0.013	−0.008	0.026	0.007	−0.017	0.027	0.000
	0.57	0.17	0.09	0.26	0.84	0.64	0.11	0.39	0.84	0.07	0.54
CP6	−0.014	0.021	0.051	0.020	0.031	−0.025	0.020	−0.024	0.024	0.017	−0.028
	0.61	0.14	0.03	0.17	0.046	0.69	0.23	0.67	0.01	0.31	0.66
Alpha (8–12 Hz)											
P4	0.019	0.012	0.047	0.051	0.053	0.009	0.040	0.012	0.019	0.030	0.017
	0.25	0.32	0.08	0.09	0.04	0.37	0.13	0.32	0.34	0.21	0.29
P8	0.014	−0.003	0.042	−0.008	0.010	−0.028	0.008	0.007	0.034	0.041	0.009
	0.37	0.53	0.04	0.62	0.38	0.87	0.40	0.39	0.10	0.12	0.32
CP6	−0.006	0.016	0.044	0.044	0.021	−0.031	0.048	−0.014	0.018	0.046	−0.007
	0.60	0.26	0.045	0.03	0.23	0.89	0.10	0.59	0.27	0.18	0.55
Low beta (12–20Hz)											
P4	−0.005	0.001	0.023	0.016	0.024	−0.024	0.033	−0.029	−0.005	0.014	−0.015
	0.56	0.45	0.05	0.17	0.06	0.97	0.20	0.88	0.67	0.34	0.66
P8	−0.007	0.012	0.005	0.001	0.000	0.007	−0.006	−0.007	0.012	−0.006	−0.017
	0.63	0.07	0.33	0.48	0.51	0.30	0.67	0.67	0.15	0.63	0.89
CP6	−0.008	0.015	0.022	0.019	0.022	−0.025	0.017	−0.038	0.009	0.005	−0.045
	0.57	0.26	0.02	0.03	0.05	0.88	0.19	0.85	0.22	0.43	0.90
High beta (20–30 Hz)											
P4	−0.011	−0.002	0.024	−0.008	0.034	−0.020	0.012	−0.040	−0.007	0.038	−0.029
	0.62	0.52	0.08	0.61	0.11	0.77	0.39	0.85	0.61	0.23	0.74
P8	0.029	0.021	−0.003	0.014	0.019	−0.002	0.008	0.004	−0.018	0.022	−0.023
	0.26	0.15	0.55	0.16	0.12	0.54	0.21	0.36	0.76	0.24	0.94
CP6	−0.002	0.032	0.012	0.033	0.030	−0.012	0.043	−0.021	−0.008	0.028	−0.034
	0.53	0.09	0.30	0.04	0.07	0.65	0.03	0.64	0.64	0.25	0.72
Gamma (30–50 Hz)											
P4	−0.005	0.015	0.036	0.021	0.051	0.002	0.028	−0.034	0.017	0.050	0.002
	0.52	0.33	0.19	0.32	0.08	0.48	0.30	0.74	0.25	0.22	0.48
P8	0.021	0.012	0.001	0.001	0.008	−0.011	−0.012	−0.010	−0.015	0.010	−0.023
	0.34	0.38	0.54	0.45	0.31	0.63	0.90	0.69	0.70	0.34	0.85
CP6	0.015	0.036	0.048	0.044	0.035	0.003	0.036	−0.028	0.002	0.042	−0.033
	0.39	0.11	0.14	0.08	0.11	0.46	0.22	0.68	0.45	0.24	0.72

The value above in each cell corresponds to the difference between rTMS SRCoh and Sham SRCoh while the value below refers to the exact p-value obtained. Significant results are highlighted in red bold font.



tests on SRCoh data (rTMS SRCoh vs. Sham SRCoh) for each electrode pair in the six different frequency bands considered. As expected from the literature (e.g., Capotosto et al., 2014), intra-hemispheric coherence was in mean higher (0.068) than the inter-hemispheric coherence (0.037). This was evident both in general and for the single frequency bands where coherence values were found significant in both electrode-pair arrangements: theta (intra: 0.042; inter: 0.036), alpha (intra: 0.062; inter: 0.043), low beta (intra: 0.064; inter: 0.020), and high beta (intra: 0.100; inter: 0.035).

Figure 3 summarizes the significant effects in terms of coherence change due to active vs. sham stimulation of the right hemisphere and provides a clear topographical representation of such effects. Interestingly, intra- and inter-hemispheric coherence increase behaved in a different manner with respect to the frequency bands: the former decreased while the latter increased as the frequency band increased (Figure 3A).

4 Discussion

The present study investigated the effects of repetitive transcranial magnetic stimulation (rTMS) on functional

connectivity through coherence in the brain using EEG. The results contribute to our understanding of the neural mechanisms underlying the therapeutic effects of rTMS and its potential application in stroke rehabilitation. Specifically, we investigated intra- and inter-hemispheric coherence changes induced by rTMS of rPPC. Healthy participants were administered with a 30 min of low frequency (1Hz) rTMS protocol, which has been shown to reduce neural excitability (Chen et al., 1997; Borojerdj et al., 2000), while resting-state EEG signal was recorded before and after rTMS. The main goal of the present investigation was to uncover the networks of areas functionally interconnected with the stimulated (rPPC) area by measuring EEG coherence. The logic was the following: higher coherence between rPPC and other distant areas would imply that these areas are functionally connected with rPPC and that their activity after rTMS is changed in the same manner (functional coupling) as the activity in rPPC. Specifically, we found that the sites showing a functional coupling (increased coherence) with rPPC after rTMS are the homologous (parietal) sites on the contralateral (left) hemisphere, in line with previous findings using TMS-evoked potentials (Bagattini et al., 2015b), and fronto-central sites within the stimulated (right)

hemisphere. Accordingly, an increase in power was found at the stimulated sites and at the contralateral homologous and frontal sites. Since the effects of this rTMS protocol applied to rPPC have been assessed to be inhibitory by directly measuring cortical reactivity (Bagattini et al., 2015b), we can infer that, after rTMS, sites showing high coherence with rPPC are inhibited as well, i.e., they have a reduced cortical reactivity.

These results have implications both for basic knowledge about how different areas are functionally connected and for the possibility of applying this knowledge to the field of rehabilitation after brain damage. Firstly, they reveal a network of functionally coupled areas, both within and between hemispheres, oscillating coherently. Specifically, the present results revealed a functionally coupled fronto-parietal network within the right hemisphere, a network that has been found to be relevant for several cognitive functions (Marek and Dosenbach, 2018), such as for example attentional performance (Fellrath et al., 2016; Rogala et al., 2020), visuo-motor processes (Naranjo et al., 2006; Iturrate et al., 2018), visuospatial judgement (Guidali et al., 2023), and working memory and cognitive control (Gulbinaite et al., 2014; Bertaccini et al., 2022). Moreover, results have shown a functional coupling among homologous sites in the two hemispheres which are, thus, found to be connected in an excitatory manner, in line with previous research with different neuroimaging techniques in both healthy participants and neglect patients (Ricci et al., 2012; Bagattini et al., 2015b; Lunven et al., 2015; Killington et al., 2016; Ptak et al., 2020; Schintu et al., 2020, 2021). Importantly, cortico-cortical connectivity changes induced by TMS on resting-state connectivity MRI (Fox et al., 2012) have also been investigated. These studies have shown to be a powerful tool to reveal complex patterns of network modulation both within and across hemispheres. Unfortunately though, very few TMS protocols have been applied to areas other than the motor cortex (Han et al., 2023). Since network changes induced by TMS are specific for the stimulated area (Castrillon et al., 2020), a direct comparison with the present data lacks conclusive power. To our knowledge, the study most similar to the one presented here relates to a recently published TMS-EEG and MRI integrated approach (Esposito et al., 2022). In this study, the authors applied TMS, among other areas, to the right parietal cortex and analyzed structural and functional connectivity of the default mode network. The results have shown strong functional coupling of the right parietal sites with the homologous left parietal sites and with the fronto-central sites, in agreement with the present data. More research is needed to obtain a clearer picture of the complexity of cortico-cortical connectivity changes induced by TMS.

Interestingly, results also show higher inter-hemispheric coherence for low-frequency bands and higher intra-hemispheric coherence for high-frequency bands which can be explained by the underlying neural mechanisms and functional connectivity patterns in the brain (Varela et al., 2001; Buzsáki and Draguhn, 2004; Fries, 2015). Indeed, frequency power spectrum is topographically organized as a gradient along the antero-posterior axis: lower frequency bands dominate at back of the brain while higher frequency bands dominate at frontal sites (Niedermeyer, 1999). It is, thus, more likely that, by applying rTMS over the rPPC, more inter-hemispheric coherence can be found

between posterior pairs of electrodes at low frequency bands. In the same vein, an increase of intra-hemispheric coherence for higher frequency bands is expected along the fronto-parietal network within the stimulated (right) hemisphere. Moreover, low-frequency bands, such as delta and theta waves, are associated with slower oscillations and are believed to reflect long-range connectivity and coordination between brain regions. These slow waves facilitate communication and synchronization between distant brain areas, including inter-hemispheric connections. Therefore, higher inter-hemispheric coherence in low-frequency bands suggests stronger coordination and information exchange between the two hemispheres. Consistently, a recent study showed that theta band effective inter-hemispheric connectivity between parietal regions sustained the leftward visuospatial advantage typically observed in neurologically healthy individuals (Bagattini et al., 2022). On the other hand, high-frequency bands, such as beta and gamma waves, are associated with faster oscillations and are believed to reflect local processing and information integration within specific brain regions. These fast waves are important for intra-hemispheric communication and are involved in various cognitive functions. Therefore, higher intra-hemispheric coherence in high-frequency bands indicates enhanced local processing and functional integration within each hemisphere.

Importantly, the present results provide implications for stroke rehabilitation, particularly addressing cognitive deficits such as neglect. Indeed, previous research has demonstrated the efficacy of contralesional low-frequency rTMS in reducing symptoms associated with these conditions. However, the neural mechanisms underlying these improvements have not been fully understood. The present study, by revealing the network of functionally connected areas engaged by rTMS and the nature of this connection, provided insights into the interplay between the hemispheres and the potential mechanisms underlying the genesis of the chronicity of symptoms. Specifically, the notion of the hyperactivity of the left hemisphere as a consequence of the release from the inhibition exerted by the right hemisphere (Kinsbourne, 1977) may not be the primary cause of the genesis of neglect symptoms. Rehabilitation protocols based on this notion, thus, may not be effective in reducing neglect symptoms in the long term (Müri et al., 2013; Carter and Barrett, 2023). Conversely, these data and those already present in literature on neglect patients could serve in devising *ah-hoc* protocols taking into account the complex interplay of intra- and inter-hemispheric networks abnormalities in neglect patients (Bartolomeo, 2014, 2019, 2021; Bartolomeo and Thiebaut de Schotten, 2016). Indeed, the hyperactivity in the left hemisphere of neglect patients could be the result of maladaptive plasticity (Nava and Röder, 2011; Altman et al., 2019) following brain lesion and not as the cause of the breakdown of the reciprocal inhibition exerts by the two hemispheres, which seems to be an oversimplification of brain dynamics (Berlucchi, 1983; Ptak et al., 2020). Accordingly, contralesional hyperactivity may not be adequate as the only determinant to implement rehabilitation protocols. Indeed, imaging studies have found no signs of hyperactivity in the left hemisphere of neglect patients tested in the acute phase (Vallar et al., 1988; Fiorelli et al., 1991; Perani et al., 1993; Umarova et al., 2011, 2014) whereas right hemisphere fronto-parietal network activity has been shown to

predict neglect's severity (Corbetta and Shulman, 2002; He et al., 2007; Carter et al., 2010; Machner et al., 2020). These pieces of evidence, thus, support the conclusion that the reinstatement of neural functionality in both the left and right hemispheres contributes as a predictor of functional recovery from neglect (Corbetta et al., 2005; Cramer, 2008; Lunven et al., 2015; Umarova et al., 2016).

In conclusion, the study demonstrated that inhibitory rTMS applied to the right posterior parietal cortex modulated functional connectivity and coherence in the brain. The findings challenge the notion of reciprocal inhibition between the hemispheres and suggest a role for maladaptive plasticity in spatial neglect. The study's approach of investigating non-motor areas provides valuable insights into the intra- and inter-hemispheric effects of rTMS and its potential as a therapeutic intervention in stroke rehabilitation. Further research with larger sample sizes and stroke patients is warranted to confirm and expand upon these findings.

Data availability statement

The datasets presented in this study can be found in online repositories. The names of the repository/repositories and accession number(s) can be found below: <https://doi.org/10.17605/OSF.IO/4VHM7>.

Ethics statement

The studies involving humans were approved by Ethical Committee of the Department of Neuroscience, Biomedicine and Movement Sciences. The studies were conducted in accordance with the local legislation and institutional requirements. The participants provided their written informed consent to participate in this study.

Author contributions

CM: Data curation, Formal analysis, Methodology, Software, Supervision, Validation, Visualization, Writing – review & editing, Investigation, Writing – original draft. SM: Data curation, Methodology, Supervision, Validation, Visualization, Writing – review & editing, Investigation, Software. CB: Supervision, Validation, Visualization, Writing – review & editing, Data curation, Investigation, Methodology, Software. JS-L: Supervision, Validation, Visualization, Writing – review & editing, Data curation, Investigation, Methodology, Software. SS: Methodology, Software, Supervision, Validation, Visualization, Writing –

review & editing, Conceptualization, Funding acquisition, Project administration, Writing – original draft.

Funding

The author(s) declare that financial support was received for the research, authorship, and/or publication of this article. Work supported by #NEXTGENERATIONEU (NGEU) and funded by the Ministry of University and Research (MUR), National Recovery and Resilience Plan (NRRP), project MNESYS (PE0000006)—“A Multiscale integrated approach to the study of the nervous system in health and disease” (DN. 1553 11.10.2022); MIUR PRIN 2017, “From brain dynamics to restoration of visual awareness after damage to the visual cortex.” grant no. 2017TBA4KS_002; Fondazione Cassa di Risparmio di Verona, Vicenza, Belluno e Ancona “Ricerca scientifica d'eccellenza 2018”, “Emergence of Consciousness: From neural dynamics to complex conscious behavior” grant no. 2018.0861; and CM was supported by MIUR D.M. 737/2021—“Neural correlates of perceptual awareness: from neural architecture to the preservation of conscious vision in brain tumor patients”.

Conflict of interest

The authors declare that the research was conducted in the absence of any commercial or financial relationships that could be construed as a potential conflict of interest.

The author(s) declared that they were an editorial board member of Frontiers, at the time of submission. This had no impact on the peer review process and the final decision.

Publisher's note

All claims expressed in this article are solely those of the authors and do not necessarily represent those of their affiliated organizations, or those of the publisher, the editors and the reviewers. Any product that may be evaluated in this article, or claim that may be made by its manufacturer, is not guaranteed or endorsed by the publisher.

Supplementary material

The Supplementary Material for this article can be found online at: <https://www.frontiersin.org/articles/10.3389/fnhum.2024.1362742/full#supplementary-material>

References

- Altman, K., Shavit-Stein, E., and Maggio, N. (2019). Post stroke seizures and epilepsy: from proteases to maladaptive plasticity. *Front. Cell. Neurosci.* 13:478811. doi: 10.3389/fncel.2019.00397
- Ambrosini, E., Capizzi, M., Arbula, S., and Vallesi, A. (2020). Right-lateralized intrinsic brain dynamics predict monitoring abilities. *Cogn. Affect. Behav. Neurosci.* 20, 294–308. doi: 10.3758/s13415-020-00769-6

- Bagattini, C., Esposito, M., Ferrari, C., Mazza, V., and Brignani, D. (2022). Connectivity alterations underlying the breakdown of pseudoneglect: new insights from healthy and pathological aging. *Front. Aging Neurosci.* 14:930877. doi: 10.3389/fnagi.2022.930877
- Bagattini, C., Mazzi, C., and Savazzi, S. (2015a). Waves of awareness for occipital and parietal phosphene perception. *Neuropsychologia*. doi: 10.1016/j.neuropsychologia.2015.02.021
- Bagattini, C., Mele, S., Brignani, D., and Savazzi, S. (2015b). No causal effect of left hemisphere hyperactivity in the genesis of neglect-like behavior. *Neuropsychologia* 72, 12–21. doi: 10.1016/j.neuropsychologia.2015.04.010
- Bartolomeo, P. (2014). “Spatially biased decisions: toward a dynamic interactive model of visual neglect,” in *Cognitive Plasticity in Neurologic Disorders*, eds J. I. Tracy, B. M. Hampstead, and K. Sathian (Oxford: Oxford University Press), 299–322.
- Bartolomeo, P. (2019). Visual neglect: getting the hemispheres to talk to each other. *Brain* 142, 840–842. doi: 10.1093/brain/awz043
- Bartolomeo, P. (2021). From competition to cooperation: visual neglect across the hemispheres. *Rev. Neurol.* 177, 1104–1111. doi: 10.1016/j.neuro.2021.07.015
- Bartolomeo, P., and Thiebaut de Schotten, M. (2016). Let thy left brain know what thy right brain doeth: inter-hemispheric compensation of functional deficits after brain damage. *Neuropsychologia* 93(Pt. B), 407–412. doi: 10.1016/j.neuropsychologia.2016.06.016
- Berger, H. (1929). Über das Elektroenkephalogramm des Menschen. *Arch. Psychiatr.* 87, 527–570. doi: 10.1007/BF01797193
- Berlucchi, G. (1983). Two hemispheres but one brain. *Behav. Brain Sci.* 6, 171–172. doi: 10.1017/S0140525X0001534X
- Bertaccini, R., Ellena, G., Macedo-Pascual, J., Carusi, F., Trajkovic, J., Poch, C., et al. (2022). Parietal alpha oscillatory peak frequency mediates the effect of practice on visuospatial working memory performance. *Vision* 6:30. doi: 10.3390/vision6020030
- Borojerd, B., Prager, A., Muellbacher, W., and Cohen, L. G. (2000). Reduction of human visual cortex excitability using 1-Hz transcranial magnetic stimulation. *Neurology* 54, 1529–1531. doi: 10.1212/WNL.54.7.1529
- Bortoletto, M., Veniero, D., Thut, G., and Miniussi, C. (2015). The contribution of TMS-EEG coregistration in the exploration of the human cortical connectome. *Neurosci. Biobehav. Rev.* 49, 114–124. doi: 10.1016/j.neubiorev.2014.12.014
- Brighina, F., Bisiach, E., Piazza, A., Oliveri, M., La Bua, V., Daniele, O., et al. (2002). Perceptual and response bias in visuospatial neglect due to frontal and parietal repetitive transcranial magnetic stimulation in normal subjects. *Neuroreport* 13, 2571–2575. doi: 10.1097/00001756-200212200-00038
- Buzsáki, G., and Draguhn, A. (2004). Neuronal oscillations in cortical networks. *Science* (80-) 304, 1926–1929. doi: 10.1126/science.1099745
- Capotosto, P., Babiloni, C., Romani, G. L., and Corbetta, M. (2014). Resting-state modulation of alpha rhythms by interference with angular gyrus activity. *J. Cogn. Neurosci.* 26, 107–119. doi: 10.1162/jocn_a_00460
- Carter, A. R., Astafiev, S. V., Lang, C. E., Connor, L. T., Rengachary, J., Strube, M. J., et al. (2010). Resting interhemispheric functional magnetic resonance imaging connectivity predicts performance after stroke. *Ann. Neurol.* 67, 365–375. doi: 10.1002/ana.21905
- Carter, A. R., and Barrett, A. M. (2023). Recent advances in treatment of spatial neglect: networks and neuropsychology. *Expert Rev. Neurother.* 23, 587–601. doi: 10.1080/14737175.2023.2221788
- Castrillon, G., Sollmann, N., Kurcys, K., Razi, A., Krieg, S. M., and Riedl, V. (2020). The physiological effects of noninvasive brain stimulation fundamentally differ across the human cortex. *Sci. Adv.* 6:aay2739. doi: 10.1126/sciadv.aay2739
- Chen, R., Classen, J., Gerloff, C., Celnik, P., Wassermann, E. M., Hallett, M., et al. (1997). Depression of motor cortex excitability by low-frequency transcranial magnetic stimulation. *Neurology* 48, 1398–1403. doi: 10.1212/WNL.48.5.1398
- Chen, W. H., Mima, T., Siebner, H. R., Oga, T., Hara, H., Satow, T., et al. (2003). Low-frequency rTMS over lateral premotor cortex induces lasting changes in regional activation and functional coupling of cortical motor areas. *Clin. Neurophysiol.* 114, 1628–1637. doi: 10.1016/S1388-2457(03)00063-4
- Corbetta, M., Kincade, M. J., Lewis, C., Snyder, A. Z., and Sapir, A. (2005). Neural basis and recovery of spatial attention deficits in spatial neglect. *Nat. Neurosci.* 8, 1603–1610. doi: 10.1038/nn1574
- Corbetta, M., and Shulman, G. L. (2002). Control of goal-directed and stimulus-driven attention in the brain. *Nat. Rev. Neurosci.* 3, 201–215. doi: 10.1038/nrn755
- Cramer, S. C. (2008). Repairing the human brain after stroke: I. Mechanisms of spontaneous recovery. *Ann. Neurol.* 63, 272–287. doi: 10.1002/ana.21393
- Efron, B., and Tibshirani, R. J. (1993). An introduction to the bootstrap. *Refriger. Air Cond.* 57, 436. doi: 10.1007/978-1-4899-4541-9
- Esposito, R., Bortoletto, M., Zaccà, D., Avesani, P., and Miniussi, C. (2022). An integrated TMS-EEG and MRI approach to explore the interregional connectivity of the default mode network. *Brain Struct. Funct.* 227, 1133–1144. doi: 10.1007/s00429-022-02453-6
- Fein, G., Raz, J., Brown, F. F., and Merrin, E. L. (1988). Common reference coherence data are confounded by power and phase effects. *Electroencephalogr. Clin. Neurophysiol.* 69, 581–584. doi: 10.1016/0013-4694(88)90171-X
- Fellrath, J., Mottaz, A., Schnider, A., Guggisberg, A. G., and Ptak, R. (2016). Theta-band functional connectivity in the dorsal fronto-parietal network predicts goal-directed attention. *Neuropsychologia* 92, 20–30. doi: 10.1016/j.neuropsychologia.2016.07.012
- Fierro, B., Brighina, F., Oliveri, M., Piazza, A., La Bua, V., Buffa, D., et al. (2000). Contralateral neglect induced by right posterior parietal rTMS in healthy subjects. *Neuroreport* 11, 1519–1521. doi: 10.1097/00001756-200005150-00031
- Fiorelli, M., Blin, J., Bakchine, S., Laplane, D., and Baron, J. C. (1991). PET studies of cortical diaschisis in patients with motor hemi-neglect. *J. Neuro. Sci.* 104, 135–142. doi: 10.1016/0022-510X(91)90302-N
- Fox, M. D., Halko, M. A., Eldaief, M. C., and Pascual-Leone, A. (2012). Measuring and manipulating brain connectivity with resting state functional connectivity magnetic resonance imaging (fcMRI) and transcranial magnetic stimulation (TMS). *Neuroimage* 62, 2232–2243. doi: 10.1016/j.neuroimage.2012.03.035
- Fries, P. (2005). A mechanism for cognitive dynamics: neuronal communication through neuronal coherence. *Trends Cogn. Sci.* 9, 474–480. doi: 10.1016/j.tics.2005.08.011
- Fries, P. (2015). Rhythms for cognition: communication through coherence. *Neuron* 88, 220–235. doi: 10.1016/j.neuron.2015.09.034
- Gainotti, G. (2015). Contrasting opinions on the role of the right hemisphere in the recovery of language. A critical survey. *Aphasiology* 29, 1020–1037. doi: 10.1080/02687038.2015.1027170
- Gerloff, C., Richard, J., Hadley, J., Schulman, A. E., Honda, M., and Hallett, M. (1998). Functional coupling and regional activation of human cortical motor areas during simple, internally paced and externally paced finger movements. *Brain* 121, 1513–1531. doi: 10.1093/brain/121.8.1513
- Grieder, M., and Koenig, T. (2023). Effect of Acoustic fMRI-Scanner Noise on the Human Resting State. *Brain Topogr.* 36, 32–41. doi: 10.1007/s10548-022-00933-w
- Guidali, G., Bagattini, C., De Matola, M., and Brignani, D. (2023). Influence of frontal-to-parietal connectivity in pseudoneglect: a cortico-cortical paired associative stimulation study. *Cortex* 169, 50–64. doi: 10.1016/j.cortex.2023.08.012
- Gulbinaite, R., van Rijn, H., and Cohen, M. X. (2014). Fronto-parietal network oscillations reveal relationship between working memory capacity and cognitive control. *Front. Hum. Neurosci.* 8:761. doi: 10.3389/fnhum.2014.00761
- Han, X., Zhu, Z., Luan, J., Lv, P., Xin, X., Zhang, X., et al. (2023). Effects of repetitive transcranial magnetic stimulation and their underlying neural mechanisms evaluated with magnetic resonance imaging-based brain connectivity network analyses. *Eur. J. Radiol. Open* 10:100495. doi: 10.1016/j.ejro.2023.100495
- He, B. J., Snyder, A. Z., Vincent, J. L., Epstein, A., Shulman, G. L., and Corbetta, M. (2007). Breakdown of functional connectivity in frontoparietal networks underlies behavioral deficits in spatial neglect. *Neuron* 53, 905–918. doi: 10.1016/j.neuron.2007.02.013
- Heilman, K. M., and Valenstein, E. (1979). Mechanisms underlying hemispatial neglect. *Ann. Neurol.* 5, 166–170. doi: 10.1002/ana.410050210
- Hesse, M. D., Sparing, R., and Fink, G. R. (2011). Ameliorating spatial neglect with non-invasive brain stimulation: from pathophysiological concepts to novel treatment strategies. *Neuropsychol. Rehabil.* 21, 676–702. doi: 10.1080/09602011.2011.573931
- Hummel, F., Andres, F., Altenmüller, E., Dichgans, J., and Gerloff, C. (2002). Inhibitory control of acquired motor programmes in the human brain. *Brain* 125, 404–420. doi: 10.1093/brain/awf030
- Ilmoniemi, R. J., Virtanen, J., Ruohonen, J., Karhu, J., Aronen, H. J., Näätänen, R., et al. (1997). Neuronal responses to magnetic stimulation reveal cortical reactivity and connectivity. *Neuroreport* 8, 3537–3540. doi: 10.1097/00001756-199711100-00024
- Iturrate, I., Chavarriaga, R., Pereira, M., Zhang, H., Corbet, T., Leeb, R., et al. (2018). Human EEG reveals distinct neural correlates of power and precision grasping types. *Neuroimage* 181, 635–644. doi: 10.1016/j.neuroimage.2018.07.055
- Jacquin-Courtois, S. (2015). Hemi-spatial neglect rehabilitation using non-invasive brain stimulation: or how to modulate the disconnection syndrome? *Ann. Phys. Rehabil. Med.* 58, 251–258. doi: 10.1016/j.rehab.2015.07.388
- Jamieson, G. A., and Burgess, A. P. (2014). Hypnotic induction is followed by state-like changes in the organization of EEG functional connectivity in the theta and beta frequency bands in high-hypnotically susceptible individuals. *Front. Hum. Neurosci.* 8:86859. doi: 10.3389/fnhum.2014.00528
- Kam, J. W. Y., Bolbecker, A. R., O'Donnell, B. F., Hetrick, W. P., and Brenner, C. A. (2013). Resting state EEG power and coherence abnormalities in bipolar disorder and schizophrenia. *J. Psychiatr. Res.* 47, 1893–1901. doi: 10.1016/j.jpsychires.2013.09.009
- Killington, C., Barr, C., Loetscher, T., and Bradnam, L. V. (2016). Variation in left posterior parietal-motor cortex interhemispheric facilitation following right parietal continuous theta-burst stimulation in healthy adults. *Neuroscience* 330, 229–235. doi: 10.1016/j.neuroscience.2016.05.056
- Kinsbourne, M. (1977). Hemi-neglect and hemisphere rivalry. *Adv. Neurol.* 18, 41–49.

- Koch, G., Cercignani, M., Bonni, S., Giacobbe, V., Bucchi, G., Versace, V., et al. (2011). Asymmetry of parietal interhemispheric connections in humans. *J. Neurosci.* 31, 8967–8975. doi: 10.1523/JNEUROSCI.6567-10.2011
- Koch, G., Oliveri, M., Cheeran, B., Ruge, D., Gerfo, E., Lo Salerno, S., et al. (2008). Hyperexcitability of parietal-motor functional connections in the intact left-hemisphere of patients with neglect. *Brain* 131, 3147–3155. doi: 10.1093/brain/awn273
- Koch, G., Veniero, D., and Caltagirone, C. (2013). To the other side of the neglected brain: the hyperexcitability of the left intact hemisphere. *Neuroscientist* 19, 208–217. doi: 10.1177/1073858412447874
- Lunven, M., De Schotten, M. T., Bourlon, C., Duret, C., Migliaccio, R., Rode, G., et al. (2015). White matter lesional predictors of chronic visual neglect: a longitudinal study. *Brain* 138, 746–760. doi: 10.1093/brain/awu389
- Machner, B., von der Gabelntz, J., Göttlich, M., Heide, W., Helmchen, C., Sprenger, A., et al. (2020). Behavioral deficits in left hemispatial neglect are related to a reduction of spontaneous neuronal activity in the right superior parietal lobule. *Neuropsychologia* 138:107356. doi: 10.1016/j.neuropsychologia.2020.107356
- Maeda, F., Keenan, J. P., Tormos, J. M., Topka, H., and Pascual-Leone, A. (2000). Interindividual variability of the modulatory effects of repetitive transcranial magnetic stimulation on cortical excitability. *Exp. Brain Res.* 133, 425–430. doi: 10.1007/s002210000432
- Marek, S., and Dosenbach, N. U. F. (2018). The frontoparietal network: function, electrophysiology, and importance of individual precision mapping. *Dialogues Clin. Neurosci.* 20:133. doi: 10.31887/DCNS.2018.20.2/smarek
- Mazzi, C., Mazzeo, G., and Savazzi, S. (2017). Markers of TMS-evoked visual conscious experience in a patient with altitudinal hemianopia. *Conscious. Cogn.* 54, 143–154. doi: 10.1016/j.concog.2017.01.022
- Miniussi, C., Harris, J. A., and Ruzzoli, M. (2013). Modelling non-invasive brain stimulation in cognitive neuroscience. *Neurosci. Biobehav. Rev.* 37, 1702–1712. doi: 10.1016/j.neubiorev.2013.06.014
- Miniussi, C., and Thut, G. (2010). Combining TMS and EEG offers new prospects in cognitive neuroscience. *Brain Topogr.* 22, 249–256. doi: 10.1007/s10548-009-0083-8
- Müri, R. M., Cazzoli, D., Nef, T., Mosimann, U. P., Hopfner, S., and Nyffeler, T. (2013). Non-invasive brain stimulation in neglect rehabilitation: an update. *Front. Hum. Neurosci.* 7:248. doi: 10.3389/fnhum.2013.00248
- Naranjo, J. R., Brovelli, A., Longo, R., Budai, R., Kristeva, R., and Battaglini, P. P. (2006). EEG dynamics of the frontoparietal network during reaching preparation in humans. *Neuroimage* 34, 1673–1682. doi: 10.1016/j.neuroimage.2006.07.049
- Nava, E., and Röder, B. (2011). Adaptation and maladaptation: insights from brain plasticity. *Prog. Brain Res.* 191, 177–194. doi: 10.1016/B978-0-444-53752-2.00005-9
- Neuhaus, E., Lowry, S. J., Santhosh, M., Kresse, A., Edwards, L. A., Keller, J., et al. (2021). Resting state EEG in youth with ASD: age, sex, and relation to phenotype. *J. Neurodev. Disord.* 13, 1–15. doi: 10.1186/s11689-021-09390-1
- Niedermeyer, E. (1999). “The normal EEG of the waking adult,” in *Electroencephalography: Basic Principles, Clinical Applications and Related Fields*, eds E. Niedermeyer, and F. Lopes da Silva (Baltimore, MD: Lippincott Williams and Wilkins), 149–173.
- Nunez, P. L., Srinivasan, R., Westdorp, A. F., Wijesinghe, R. S., Tucker, D. M., Silberstein, R. B., et al. (1997). EEG coherency. I: Statistics, reference electrode, volume conduction, Laplacians, cortical imaging, and interpretation at multiple scales. *Electroencephalogr. Clin. Neurophysiol.* 103, 499–515. doi: 10.1016/S0013-4694(97)00066-7
- Oldfield, R. C. (1971). The assessment and analysis of handedness: the Edinburgh inventory. *Neuropsychologia* 9, 97–113. doi: 10.1016/0028-3932(71)90067-4
- Oliveri, M. (2011). Brain stimulation procedures for treatment of contralateral spatial neglect. *Restor. Neurol. Neurosci.* 29, 421–425. doi: 10.3233/RNN-2011-0613
- Oruç, I., Krigolson, O., Dalrymple, K., Nagamatsu, L. S., Handy, T. C., and Barton, J. S. (2011). Bootstrap analysis of the single subject with event related potentials. *Cogn. Neuropsychol.* 28, 322–337. doi: 10.1080/02643294.2011.648176
- Perani, D., Vallar, G., Paulesu, E., Alberoni, M., and Fazio, F. (1993). Left and right hemisphere contribution to recovery from neglect after right hemisphere damage—an [18F]FDG pet study of two cases. *Neuropsychologia* 31, 115–125. doi: 10.1016/0028-3932(93)90040-7
- Perrin, F., Pernier, J., and Bertrand, O. E. J. (1989). Spherical splines for scalp potential and current density mapping. *Electroencephalogr. Clin. Neurophysiol.* 72, 184–187. doi: 10.1016/0013-4694(89)90180-6
- Pfurtscheller, G., and Lopes da Silva, F. (1999). Event-related EEG/MEG synchronization and desynchronization: basic principles. *Clin. Neurophysiol.* 110, 1842–1857. doi: 10.1016/S1388-2457(99)00141-8
- Pia, L., Neppi-Modona, M., Rosselli, F. B., Muscatello, V., Rosato, R., and Ricci, R. (2012). The Opperl-Kundt illusion is effective in modulating horizontal space representation in humans 1,2. *Percept. Mot. Skills* 115, 729–742. doi: 10.2466/24.22.27.PMS.115.6.729-742
- Plewnia, C., Rilk, A. J., Soekadar, S. R., Arfeller, C., Huber, H. S., Sauseng, P., et al. (2008). Enhancement of long-range EEG coherence by synchronous bifocal transcranial magnetic stimulation. *Eur. J. Neurosci.* 27, 1577–1583. doi: 10.1111/j.1460-9568.2008.06124.x
- Ptak, R., Bourgeois, A., Cavelti, S., Doganci, N., Schnider, A., and Iannotti, G. R. (2020). Discrete Patterns of cross-hemispheric functional connectivity underlie impairments of spatial cognition after stroke. *J. Neurosci.* 40:6638. doi: 10.1523/JNEUROSCI.0625-20.2020
- Ranlund, S., Nottage, J., Shaikh, M., Dutt, A., Constante, M., Walshe, M., et al. (2014). Resting EEG in psychosis and at-risk populations — A possible endophenotype? *Schizophr. Res.* 153:96. doi: 10.1016/j.schres.2013.12.017
- Rappelsberger, P., and Petsche, H. (1988). Probability mapping: power and coherence analyses of cognitive processes. *Brain Topogr.* 1, 46–54. doi: 10.1007/BF01129339
- Ricci, R., Salatino, A., Li, X., Funk, A. P., Logan, S. L., Mu, Q., et al. (2012). Imaging the neural mechanisms of TMS neglect-like bias in healthy volunteers with the interleaved TMS/fMRI technique: Preliminary evidence. *Front. Hum. Neurosci.* 6, 1–13. doi: 10.3389/fnhum.2012.00326
- Robertson, E. M., Théoret, H., and Pascual-Leone, A. (2003). Studies in cognition: the problems solved and created by transcranial magnetic stimulation. *J. Cogn. Neurosci.* 15, 948–960. doi: 10.1162/089892903770007344
- Rogala, J., Kublik, E., Krauz, R., and Wróbel, A. (2020). Resting-state EEG activity predicts frontoparietal network reconfiguration and improved attentional performance. *Sci. Rep.* 10, 1–15. doi: 10.1038/s41598-020-61866-7
- Rossi, S., Hallett, M., Rossini, P. M., and Pascual-Leone, A. (2009). Safety, ethical considerations, and application guidelines for the use of transcranial magnetic stimulation in clinical practice and research. *Clin. Neurophysiol.* 120, 2008–2039. doi: 10.1016/j.clinph.2009.08.016
- Rossi, S., Hallett, M., Rossini, P. M., and Pascual-Leone, A. (2011). Screening questionnaire before TMS: an update. *Clin. Neurophysiol.* 122:1686. doi: 10.1016/j.clinph.2010.12.037
- Rossini, P. M., Barker, A. T., Berardelli, A., Caramia, M. D., Caruso, G., Cracco, R. Q., et al. (1994). Non-invasive electrical and magnetic stimulation of the brain, spinal cord and roots: basic principles and procedures for routine clinical application. Report of an IFCN committee. *Electroencephalogr. Clin. Neurophysiol.* 91, 79–92. doi: 10.1016/0013-4694(94)90029-9
- Salatino, A., Berra, E., Troni, W., Sacco, K., Cauda, F., D’Agata, F., et al. (2014). Behavioral and neuroplastic effects of low-frequency rTMS of the unaffected hemisphere in a chronic stroke patient: a concomitant TMS and fMRI study. *Neurocase* 20, 615–626. doi: 10.1080/13554794.2013.826691
- Savazzi, S., Posteraro, L., Veronesi, G., and Mancini, F. (2007). Rightward and leftward bisection biases in spatial neglect: two sides of the same coin? *Brain* 130:awm143. doi: 10.1093/brain/awm143
- Schenkenberg, T., Bradford, D. C., and Ajax, E. T. (1980). Line bisection and unilateral visual neglect in patients with neurologic impairment. *Neurology* 30, 509–517. doi: 10.1212/WNL.30.5.509
- Schintu, S., Cunningham, C. A., Freedberg, M., Taylor, P., Gotts, S. J., Shomstein, S., et al. (2021). Callosal anisotropy predicts attentional network changes after parietal inhibitory stimulation. *Neuroimage* 226:117559. doi: 10.1016/j.neuroimage.2020.117559
- Schintu, S., Freedberg, M., Gotts, S. J., Cunningham, C. A., Alam, Z. M., Shomstein, S., et al. (2020). Prism adaptation modulates connectivity of the intraparietal sulcus with multiple brain networks. *Cereb. Cortex* 30, 4747–4758. doi: 10.1093/cercor/bhaa032
- Shah, P. P., Szaflarski, J. P., Allendorfer, J., and Hamilton, R. H. (2013). Induction of neuroplasticity and recovery in post-stroke aphasia by non-invasive brain stimulation. *Front. Hum. Neurosci.* 7:888. doi: 10.3389/fnhum.2013.00888
- Silvanto, J., and Muggleton, N. G. (2008). New light through old windows: moving beyond the “virtual lesion” approach to transcranial magnetic stimulation. *Neuroimage* 39, 549–552. doi: 10.1016/j.neuroimage.2007.09.008
- Siviero, I., Bonfanti, D., Menegaz, G., Savazzi, S., Mazzi, C., and Storti, S. F. (2023). Graph analysis of TMS-EEG connectivity reveals hemispheric differences following occipital stimulation. *Sensors* 23:8833. doi: 10.3390/s23218833
- Stokes, M. G., Chambers, C. D., Gould, I. C., Henderson, T. R., Janko, N. E., Allen, N. B., et al. (2005). Simple metric for scaling motor threshold based on scalp-cortex distance: application to studies using transcranial magnetic stimulation. *J. Neurophysiol.* 94, 4520–4527. doi: 10.1152/jn.00067.2005
- Strens, L. H. A., Oliviero, A., Bloem, B. R., Gerschlagler, W., Rothwell, J. C., and Brown, P. (2002). The effects of subthreshold 1 Hz repetitive TMS on cortico-cortical and interhemispheric coherence. *Clin. Neurophysiol.* 113, 1279–1285. doi: 10.1016/S1388-2457(02)00151-7
- Tafuro, A., Mazzi, C., and Savazzi, S. (2023). The spectral dynamics of visual awareness: an interplay of different frequencies? *Eur. J. Neurosci.* 57, 2136–2148. doi: 10.1111/ejn.15988
- Umarova, R. M., Nitschke, K., Kaller, C. P., Klöppel, S., Beume, L., Mader, I., et al. (2016). Predictors and signatures of recovery from neglect in acute stroke. *Ann. Neurol.* 79, 673–686. doi: 10.1002/ana.24614

- Umarova, R. M., Reisert, M., Beier, T. U., Kiselev, V. G., Klöppel, S., Kaller, C. P., et al. (2014). Attention-network specific alterations of structural connectivity in the undamaged white matter in acute neglect. *Hum. Brain Mapp.* 35, 4678. doi: 10.1002/hbm.22503
- Umarova, R. M., Saur, D., Kaller, C. P., Vry, M. S., Glauche, V., Mader, I., et al. (2011). Acute visual neglect and extinction: distinct functional state of the visuospatial attention system. *Brain* 134, 3310–3325. doi: 10.1093/brain/awr220
- Valero-Cabré, A., Rushmore, R. J., and Payne, B. R. (2006). Low frequency transcranial magnetic stimulation on the posterior parietal cortex induces visuotopically specific neglect-like syndrome. *Exp. Brain Res.* 172, 14–21. doi: 10.1007/s00221-005-0307-4
- Vallar, G., Perani, D., Cappa, S. F., Messa, C., Lenzi, G. L., and Fazio, F. (1988). Recovery from aphasia and neglect after subcortical stroke: neuropsychological and cerebral perfusion study. *J. Neurol. Neurosurg. Psychiatr.* 51, 1269–1276. doi: 10.1136/jnnp.51.10.1269
- Varela, F., Lachaux, J. P., Rodriguez, E., and Martinerie, J. (2001). The brainweb: phase synchronization and large-scale integration. *Nat. Rev. Neurosci.* 24, 229–239. doi: 10.1038/35067550
- Wacker, J., Dillon, D. G., and Pizzagalli, D. A. (2009). The role of the nucleus accumbens and rostral anterior cingulate cortex in anhedonia: integration of resting EEG, fMRI, and volumetric techniques. *Neuroimage* 46, 327–337. doi: 10.1016/j.neuroimage.2009.01.058
- Wang, X. J. (2010). Neurophysiological and computational principles of cortical rhythms in cognition. *Physiol. Rev.* 90, 1195–1268. doi: 10.1152/physrev.00035.2008